Mg structural state in coral aragonite and implications for the paleoenvironmental proxy

Adrian A. Finch[1] and Nicola Allison[1]

Received 6 February 2008; revised 27 February 2008; accepted 18 March 2008; published 19 April 2008.

[1] Thermodynamic calculations and inorganic precipitation experiments indicate a relationship between aragonite Mg/Ca and water temperature. This offers a route to reconstruct seawater temperatures from fossil corals. Fundamental to this is the assumption that Mg^{2+} exchanges for Ca^{2+} within carbonate. We present X-ray Absorption Fine Structure (XAFS) data to indicate the structural state of Mg in modern *Porites* coral skeletons. We show Mg is not in aragonite, but hosted by a disordered Mg-bearing material. Mg may be predominantly hosted in organic materials or as a highly disordered inorganic phase, e.g., a nanoparticulate form of Mg carbonate or hydroxide. Reported correlations between seawater temperature and coral Mg/Ca are unlikely to be consistent between corals and hence analysis of Mg/Ca in fossils is unlikely to produce accurate climate reconstructions. We anticipate XAFS will be applied widely to environmental proxies and become an important tool in identifying those that reconstruct accurate climates. **Citation:** Finch, A. A., and N. Allison (2008), Mg structural state in coral aragonite and implications for the paleoenvironmental proxy, *Geophys. Res. Lett.*, *35*, L08704, doi:10.1029/2008GL033543.

1. Introduction

[2] Correlations between the trace element geochemistry of biogenic carbonates and environmental variables form the basis for the development of paleoceanographic proxies and offer a route to reconstruct past climates from fossil specimens. Initial studies indicated the potential of Mg in aragonitic coral skeletons as a paleothermometer [e.g., *Mitsuguchi et al.*, 1996; *Sinclair et al.*, 1998; *Fallon et al.*, 1999]. However some subsequent studies reported poor correlations between skeletal Mg/Ca and sea surface temperatures (SSTs) [e.g., *Quinn and Sampson*, 2002] and the development of this paleothermometer has been undermined by some ambiguity over the controls on skeletal Mg incorporation. For example, Mg/Ca and precipitating water temperature are positively correlated in coral skeletons [e.g., *Mitsuguchi et al.*, 1996] but negatively correlated in inorganically precipitated aragonite [*Gaetani and Cohen*, 2006].

[3] The underlying assumption of Mg paleothermometry is that Mg^{2+} exchanges for Ca^{2+} within the carbonate lattice and that the substitution is temperature dependent in a manner that can be modeled consistently by inorganic partitioning between aqueous fluids and solids. However Mg and organic materials are also strongly correlated in coral skeletons at a micron scale [*Meibom et al.*, 2004; *Cuif et al.*, 2003] suggesting that Mg may not substitute for Ca in the aragonite structure. To explore the mode of Mg incorporation in coral skeletons, we have employed X-ray Absorption Fine Structure (XAFS), one of the most widely used probes of local coordination of elements in materials. XAFS examines the manner in which x-rays are absorbed by materials as a function of x-ray energy and is divided into two separate data regions called the X-ray Absorption Near Edge Structure (XANES) and the Extended X-ray Absorption Fine Structure (EXAFS). XANES is a fingerprint of a particular coordination symmetry and bonding environment, whereas EXAFS data can be processed to provide highly precise (<0.02 Å) quantitative estimates of interatomic bond distances. Using both XANES and EXAFS, the structural state of trace elements in materials can be closely determined. In this paper we report the coordination of Mg in several samples of modern *Porites* corals, the genus most commonly used for palaeoenvironmental reconstruction, from a range of localities.

2. Materials and Methods

[4] We collected Mg K-XAFS of a suite of model materials including aragonite, calcite, hydromagnesite, standard organic tissue and 7 samples of modern *Porites* corals (Table 1). XRD analysis of all corals detected aragonite as the only phase. Coral skeletons were sampled within the last ten years of growth but below the tissue layer, which contains visible organic contamination. Samples were treated with sodium chlorate(I) before analysis [*Finch and Allison*, 2003]. We measured Mg K-XAFS on Station 3.4, Daresbury Synchrotron Radiation Source (SRS), Warrington, UK. SRS is a 2 GeV machine; station 3.4 provides monochromatic x-rays between 1–3 keV. X-ray energy was standardised to a dolomite replicate (1311 eV). We measured XAFS of powders at room temperature using Mg Kα fluorescence with a solid-state detector and x-ray energies were scanned to include XANES and EXAFS. Count times were extended as energy increased to maintain signal-to-noise. The uppermost energy is constrained by Al K-absorption since Al occurs in the monochromator. Each cycle took 45 min and we averaged 2–50 cycles, more for diluter samples. Data were normalised to beam intensity and backgrounds removed. EXCURV98 was used to calculate phase-shifted Fourier transforms and to fit data to structural models using published phase shift models [*von Barth and Hedin*, 1972; *Hedin and Lundqvist*, 1969]. The coordination number (N_1) is fixed from crystallography (Table 2). The edge energy (E_f), first shell interatomic distance (R_1) and Debye-Waller parameter (A_1) were refined to minimise the

[1]School of Geography and Geosciences, University of St. Andrews, Fife, UK.

0094-8276/08/2008GL033543

Table 1. Standards and Samples Analyzed, Their Provenance, and Estimated Mg Concentration[a]

Name	Provenance	[Mg], ppm
Standards		
Magnesite ($MgCO_3$)	Mina Eugui, Navarra, Spain. Sample provided by J Garcia-Guinea, National Museum of Natural Sciences, Spain.	290,000
Dolomite ($CaMg(CO_3)_2$)	International standard ECRM 782-1, Association Nationale de la Recherche Technique, France.	128,400
Hydromagnesite ($4MgCO_3.Mg(OH)_2.4H_2O$)	BDH AnalaR Magnesium hydroxide carbonate Lot A308629	31,000
Glauconite (clay)	International standard 95-GOV-01 from Cauville, Normandy, France, Association Nationale de la Recherche Technique, France.	27,000
Organic Mg	Homogenised marine mussel, *Mytilus edulis* tissue, State Bureau of Technical Supervision, People's Republic of China, GBW 08571.	1,970
Calcite ($CaCO_3$)	Efflorescent material from roof of catacombs, Rome, Italy. Sample provided by J Garcia-Guinea, National Museum of Natural Sciences, Spain.	7,900
Aragonite ($CaCO_3$)	Minglanilla, Valencia, Spain. Sample provided by J Garcia-Guinea, National Museum of Natural Sciences, Spain.	3,000
Coral samples		
Porites lobata 1 (NA33)	Lanikai, Oahu, Hawaii	Nd
Porites lobata 2 (NA45)	Lanikai, Oahu, Hawaii (1)	950 (1)
Porites lobata 3 (Tarawa_modern)	Tarawa Atoll, W. Pacific (2)	Nd
Porites lutea 1 (JAPAN)	Shirigai Bay, Japan (3)	850[b]
Porites lutea 2 (PB3)	Phuket, Thailand (4)	Nd
Porites lutea 3 (PB4)	Phuket, Thailand (4)	Nd
Porites spp. (PNG_modern)	Huon Peninsula, Papua New Guinea (5)	770[b]

[a]All samples are confirmed as XRD phase pure; corals are phase pure aragonite. Further details on samples are given in the cited references and the names in (parentheses) below are used for that sample in those publications. Nd, not determined. Numbers in parentheses are references: 1, *Allison and Finch* [2007]; 2, *Cole et al.* [1993]; 3, *Fallon et al.* [1999]; 4, *Allison et al.* [1996]; 5, *McCulloch et al.* [1996].
[b]N. Allison (unpublished data, 2008).

squares of residuals between unfiltered data and model spectra. Multiple scattering did not improve fits. Refinements were fitted for k = 1.0–7.5 $Å^{-1}$ and R = 1–3 Å. The number of parameters supported by such data ($N = 2\Delta k\Delta R/\pi+1$) is 9.5, significantly greater than the number of variables (P = 3), giving a determinacy (N/P)>3. Performing EXAFS on short k-ranges can discriminate against the observation of longer bonds, but we observed no differences in standards refined over full and truncated k-ranges. In addition, second and third shells (up to ~4 Å) are clearly visible in the Fourier transforms of the dolomite and magnesite data (see the auxiliary material[1]) demonstrating that the bond distances obtained here are not artificially truncated by the short k-range in which we work. Analysis of calcites with different Mg concentrations confirms that EXAFS are consistent even at low concentrations [*Finch and Allison*, 2007]. Fit indices (%) relate to the $\Sigma(\text{residuals})^2 \times k^3$. Errors indicate displacements that cause a 2.5% increase in fit. The full refinements including fits of both $k^3\ \chi(k)$ and FT $k^3\ \chi(k)$ are presented in the auxiliary material.

3. Results and Discussion

[5] Mg K-edge XANES arise from electronic transitions as core 1s electrons are promoted to higher states and are extremely sensitive to local coordination [*Yoshida et al.*, 1995; *Wong et al.*, 1994]. We are able to discriminate between the XANES of all standards (Figure 1), including aragonite, calcite and organics, on the basis of subtle but consistent near-edge features. We use the XANES profiles as fingerprints of the Mg host phase. The Mg K-XANES of all the corals is featureless, indicating that Mg in the coral skeleton is surrounded by a disordered structure probably comprising elements with poor electron scattering. The Mg is not hosted predominantly by aragonite or any of the other macrocrystalline materials tested (calcite, dolomite, hydromagnesite, brucite or clays such as glauconite). Furthermore, the Mg is also not adsorbed onto aragonite surfaces. Such a structure can be modelled as Mg binding aragonite on one side but no regular structure on the other and would give XANES akin to aragonite (with the characteristic resonance) but with a dampened magnitude. The coral XANES lack this characteristic feature. In theory, featureless XANES spectra might also be generated by a complex polyphase mixture of Mg carbonates and/or hydroxides, in which resonances in one phase are offset by troughs in the XANES of other components. However, this would require an extremely unfortunate mix of materials to produce a XANES which is featureless, hence we consider it an unlikely explanation for the present data. Aqueous Mg might give similar XANES but this is also unlikely given that the samples analysed are dry powders. The XANES of the corals is consistent with those of the organic standard, a homogenised marine mussel tissue. The featureless XANES of the organic standard arises because Mg in organics is surrounded by a very variable coordination state beyond the first shell in which Mg is bound by several different molecules and/or the molecules are free to move. In proteins, Mg is locally bound to the oxygen of carboxyl groups in tetrahedral coordination [*Harding*, 2006]. Furthermore organic molecules comprise predominantly elements with poor electron backscattering (e.g., C, H) which contribute little to XANES resonances. However other structural states may produce similarly featureless XANES. These include highly disordered inorganic phases such as nanoparticulate basic Mg carbonates (in which Mg has little

[1]Auxiliary materials are available in the HTML. doi:10.1029/2008GL033543.

Table 2. Final EXAFS Refinement Parameters[a]

Standard/Sample	E_f, eV	A_1, Å^{-2}	R_1, Å	N	R, %	Mg-O by Diffraction, Å	Structural Reference
Dolomite	−4.72 ± 0.70	0.035 ± 0.008	2.087 ± 0.015	6	58.0	2.115	*Suzuki et al.* [1998]
Magnesite	−7.45 ± 0.86	0.022 ± 0.006	2.082 ± 0.014	6	62.8	2.101	*Maslen et al.* [1995]
Hydromagnesite	−4.80 ± 0.38	0.046 ± 0.005	2.068± 0.009	6	37.5	2.077	*Akao et al.* [1974]
Organic Mg	−9.64 ± 0.37	0.029 ± 0.009	2.068 ± 0.019	4	42.0	2.05 – 2.09	*Harding* [2006]
Porites lobata 1	−4.19 ± 0.75	0.012 ± 0.005	2.070 ± 0.015	4	49.0		
Porites spp.	−5.33 ± 1.24	0.018 ± 0.006	2.042 ± 0.018	4	59.3		

[a]E_f is the edge energy, A_1 the Debye-Waller factor and R_1 the interatomic Mg-O distance. N, the coordination number, is fixed and taken from the structural model. R is the fit parameter for the best refinement. The penultimate column shows the Mg-O bond distance estimated from diffraction studies. All refinements and further explanation are given in the auxiliary material.

order beyond the first shell and is bound by poorly scattering atoms such as C or H).

[6] To explore structural state further we refined the first shell Mg K-edge EXAFS of a subset of standards and corals. This process matches the observed EXAFS to a theoretical profile generated from a coordination model and provides estimates of interatomic distances around Mg and its nearest neighbor (here O). We refined the EXAFS of four Mg-rich standards (dolomite, magnesite, hydromagnesite and organically hosted Mg) against their structural models to test the accuracy of EXAFS in estimating Mg-O bond distances. Table 2 shows the final refinement parameters. The most important is the Mg-O interatomic distance (R_1). We observe good agreement between our R_1 estimates and distances determined by diffraction studies (Table 2), although the values from EXAFS are typically ∼1% shorter. Bond distances from EXAFS refinements using our methodology are accurate to within ∼0.02 Å. To obtain data with sufficient signal for EXAFS from the relatively Mg-poor corals, we summed many cycles of data collected over extended periods. Due to time constraints we limited data collection to two of the coral samples *P. lobata* 1 and *Porites spp.* 1 (each >12 hours beam time). The Mg-O bond distances all lie in a restricted range (2.04 – 2.09 Å), and there is overlap between many of the results. Hence the EXAFS does not provide good discrimination. Nevertheless, refinement of these coral EXAFS (Table 2) provides Mg-O bond distances within error of those of the organic Mg standard (2.068 ± 0.019 Å). The EXAFS data are not sufficiently robust to resolve with certainty the tetrahedral coordination of Mg in organics from octahedral coordination in carbonates and hydroxides. However, refining the data with the nine-fold coordination of aragonite provides much poorer fits and unrealistic Debye-Waller factors.

[7] Our EXAFS and XANES data show that the Mg in coral skeletons is not substituted into aragonite but is hosted by a disordered Mg-bearing material. Two hosts are credible. First, skeletal Mg may be present in an organic form. Skeletal organic matter is largely derived from the organic matrix synthesized by the coral. Endolithic organisms, e.g., algae, bacteria and fungi, and material adsorbed from ambient seawater, e.g., fulvic acids [*Boto and Isdale*, 1985] may also contribute. The exact role of the coral organic matrix in biomineralisation is unclear. The soluble component of the skeletal organic matrix contains Ca binding proteins [e.g., *Puverel et al.*, 2005]. In some corals, a meshlike network of fibres which extend across extracellular spaces from the base of the coral tissues (the calicoblastic ectoderm) to the skeleton and may act as a template for crystal formation [*Clode and Marshall*, 2003]. In other corals, no space is observed and the calicoblastic ectoderm appears to be in intimate contact with the skeleton suggesting that the calicoblastic ectoderm itself controls calcification [*Tambutte et al.*, 2007]. In either case the organic matrix plays a key role in biomineralisation. Mg regulates calcium carbonate polymorphism and morphology [e.g., *Davis et al.*, 2000] and Mg at the calcification site may

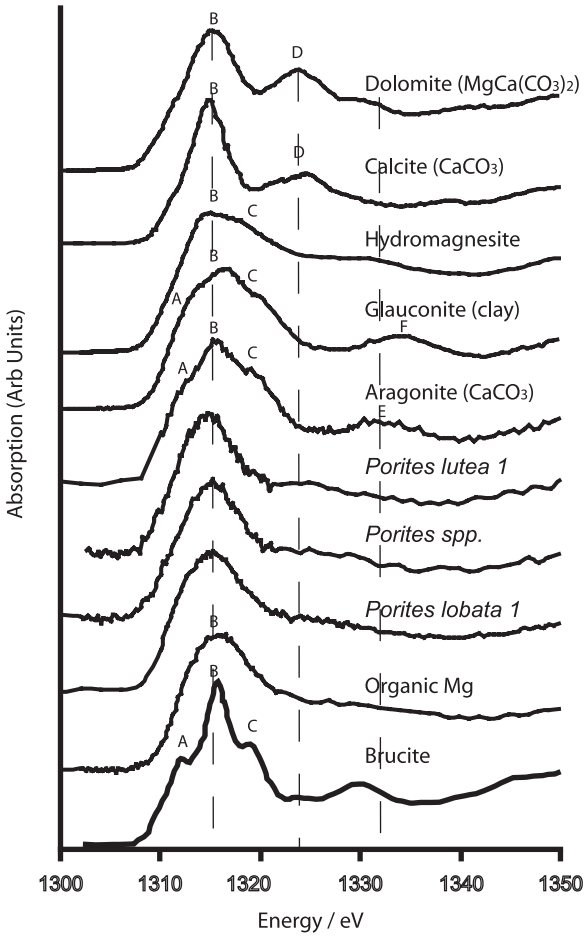

Figure 1. Mg K-XANES of model materials and three *Porites* corals. The XANES can be resolved into 6 main components given the letters A-F. Features A, B and C overlap in the edge spectrum, D characterises calcite and dolomite, E is present in aragonite and F is present in clays. The positions of the B, D and E resonances are identified by dashed lines. The profile of brucite is reproduced from [*Yoshida et al.*, 1995]. The profiles of the corals do not have E resonance that characterises aragonite and are indistinguishable from XANES of the organic Mg standard.

play a direct role in the control of biomineralisation [*Meibom et al.*, 2004]. The distributions of Mg and organic materials are well correlated in coral skeletons at a micron scale. Coral fasciculi are composed of bundles of aragonite crystals which are constructed from the repeated superimposition of growth layers a few microns thick [*Cuif et al.*, 1999]. Sulphated organic compounds [*Cuif et al.*, 2003] and Mg [*Meibom et al.*, 2004] are concentrated at the boundaries between these growth layers and in the centres of calcification which run along the approximate centers of the skeletal structures. Hydrated organics account for ~2.5% of the skeletal mass [*Cuif et al.*, 2004] and we estimate a Mg concentration of ~3.5% in this phase, if all skeletal Mg is organically complexed. Note that Mg concentrations of >1% are observed in organic rich regions of coral skeletons [*Meibom et al.*, 2004].

[8] Second, skeletal Mg may occur in a highly disordered inorganic phase. In particular we have considered the possibility that Mg may be hosted by amorphous calcium carbonate (ACC) which, although described as 'amorphous', does have short range order [*Levi-Kalisman et al.*, 2002]. ACC is difficult to detect alongside crystalline forms of calcium carbonate but plays an important role in biomineralisation in some marine phyla (see *Addadi et al.* [2003] for a review) leading to the suggestion that it is more widespread than currently appreciated. Biogenic ACC is usually associated with high Mg concentrations. EXAFS data confirm that Mg in *Porites* skeletons has short-range order, i.e. bond distances are estimated precisely (±0.02 Å) and Debye-Waller factors are similar to those in crystalline solids (Table 2). If the host is inorganic, then the featureless XANES must be a nanoparticulate material in which long-range electron resonances are absent. Such a description is consistent with ACC which has short-range order [*Levi-Kalisman et al.*, 2002] and particle sizes of ~50 nm [*Addadi et al.*, 2003]. We consider it unlikely that significant volumes of metastable ACC exist in coral skeletons given the presence of aragonite. It is more likely that ACC, if present, acts as intermediate structural state during the formation of aragonite and therefore contributes little to the volume of the skeleton. However, we are unclear what would happen to the Mg component of a transitional ACC during its transformation to aragonite. First, the Mg may simply transform with the ACC to Mg-bearing aragonite, giving the Mg XANES fingerprint observed in inorganic aragonite. Second, it may be largely released back into solution to be precipitated as another Mg-bearing mineral. Third, the Mg component of ACC may remain, forming local nanodomains of disordered Mg-bearing carbonate occluded in aragonite. The latter model is consistent with our observations.

[9] However bound, skeletal Mg is well preserved in fossil corals. Mg/Ca concentrations (2.6–3.4 mmol mol^{-1} [*Allison et al.*, 2007]) in pristine sections of Hawaiian fossil *Porites* corals (age >14 ka) are significantly lower than in their modern counterparts (~4 mmol mol^{-1} [*Allison and Finch*, 2007]), but the concentration difference is relatively small. Intracrystalline skeletal organic matter is extremely well preserved over at least century timescales [*Ingalls et al.*, 2003]. Future XAFS of fossil coral specimens will indicate the predominant mode of Mg incorporation in these skeletons.

[10] The empirical correlation of Mg/Ca and SST has met with mixed success in coral aragonite. Some corals, including one of the specimens analyzed here (*P. lutea* 1 [*Fallon et al.*, 1999]), exhibit annual Mg/Ca cyclicity that is consistent with sea surface temperatures (SSTs) while Mg/Ca in other *Porites* corals indicates no temperature dependence [e.g., *Fallon et al.*, 2003]. Our data show that the Mg is not hosted in the same phase as Ca (aragonite); hence Mg/Ca variations do not reflect partitioning between a fluid and a single mineral. Mg/Ca is controlled not just by the Mg content of the host (be it organic or nanoparticulate), but also by variations in the amount and composition of the host in the skeleton. Partitioning of Mg between fluid and nanoparticles will also depend on nanoparticle size. These collective processes, inferred to control Mg, are unlikely to be consistently described by a simple temperature dependent relationship. In reconstructing climate from fossil corals, it is assumed that the processes affecting skeletal chemistry had similar influence in the modern and fossil samples. Mg in coral skeletons is likely to reflect a complex interaction of processes which may differ between reef sites and coral specimens. Hence our data call into question the reliability of palaeoenvironmental reconstructions based on coral Mg/Ca. The application of XAFS methodologies to other proxies is required to confirm that metals substitute for Ca in the carbonate structure and to explore the reliability of other environmental proxies.

[11] **Acknowledgments.** This work is supported by NERC, UK award NER/A/S/2003/00473. Access to the Daresbury facility was provided by CCLRC, UK. Standards were provided by Javier Garcia-Guinea (National Museum of Natural Sciences, Madrid, Spain) and Angus Calder (University of St Andrews, UK). We thank Andy Smith for assistance with beam line 3.4 and Fred Mosselmans for help with the use of EXCURV98. We also thank Dan Sinclair, Scott Gaetani, Anne Cohen, Anders Meibom, and 3 anonymous reviewers for their comments on earlier drafts of this work.

References

Addadi, L., S. Raz, and S. Weiner (2003), Taking advantage of disorder: Amorphous calcium carbonate and its roles in biomineralization, *Adv. Mater.*, *15*, 959–970.

Akao, M., F. Marumo, and S. Iwai (1974), The crystal structure of hydromagnesite, *Acta Crystallogr., Sect. B*, *30*, 2670–2672.

Allison, N., and A. A. Finch (2007), High temporal resolution Mg/Ca and Ba/Ca records in modern Porites lobata corals, *Geochem. Geophys. Geosyst.*, *8*, Q05001, doi:10.1029/2006GC001477.

Allison, N., A. W. Tudhope, and A. E. Fallick (1996), A study of the factors influencing the stable carbon and oxygen isotopic composition of Porites lutea coral skeletons from Phuket, South Thailand, *Coral Reefs*, *15*, 43–57.

Allison, N., A. A. Finch, J. M. Webster, and D. A. Clague (2007), Palaeoenvironmental records from fossil corals: the effects of submarine diagenesis on temperature and climate estimates, *Geochim. Cosmochim. Acta*, *71*, 4693–4703.

Boto, K., and P. Isdale (1985), Fluorescent bands in massive corals result from terrestrial fulvic-acid inputs to nearshore zone, *Nature*, *315*, 396–397.

Cole, J. E., R. G. Fairbanks, and G. T. Shen (1993), Recent variability in the southern oscillation—Isotopic results from a Tarawa atoll coral, *Science*, *260*, 1790–1793.

Clode, P. L., and A.T. Marshall (2003), Calcium associated with a fibrillar organic matrix in the scleractinian coral Galaxea fascicularis, *Protoplasma*, *220*, 153–161.

Cuif, J. P., Y. Dauphin, and P. Gautret (1999), Compositional diversity of soluble mineralizing matrices in some recent coral skeletons compared to fine-scale growth structures of fibres: Discussion of consequences for biomineralization and diagenesis, *Int. J. Earth Sci.*, *88*, 582–592.

Cuif, J. P., Y. Dauphin, J. Doucet, M. Salome, and J. Susini (2003), XANES mapping of organic sulfate in three scleractinian coral skeletons, *Geochem. Cosmochim. Acta*, *67*, 75–83.

Cuif, J.-P., Y. Dauphin, P. Berthet, and J. Jegoudez (2004), Associated water and organic compounds in coral skeletons: Quantitative thermogravimetry coupled to infrared absorption spectrometry, *Geochem. Geophys. Geosyst.*, *5*, Q11011, doi:10.1029/2004GC000783.

Davis, K. J., P. M. Dove, and J. J. de Yoreo (2000), The role of Mg^{2+} as an impurity in calcite growth, *Science*, *290*, 1134–1137.

Fallon, S. J., M. T. McCulloch, R. van Woesik, and D. J. Sinclair (1999), Corals at their latitudinal limits: laser ablation trace element systematics in Porites from Shirigai Bay, Japan, *Earth Planet. Sci. Lett.*, *172*, 221–238.

Fallon, S. J., M. T. McCulloch, and C. Alibert (2003), Examining water temperature proxies in Porites corals from the Great Barrier Reef: A cross-shelf comparison, *Coral Reefs*, *22*, 389–404.

Finch, A. A., and N. Allison (2003), Strontium in coral aragonite: 2. Sr coordination and the long-term stability of coral environmental records, *Geochim. Cosmochim. Acta*, *67*, 4519–4527.

Finch, A. A., and N. Allison (2007), Coordination and local relaxation around Sr and Mg in calcite and aragonite, *Miner. Mag.*, *71*, 519–532.

Gaetani, G. A., and A. L. Cohen (2006), Element partitioning during precipitation of aragonite from seawater: A framework for understanding paleoproxies, *Geochim. Cosmochim. Acta*, *70*, 4617–4634.

Harding, M. M. (2006), Small revisions to predicted distances around metal sites in proteins, *Acta Crystallogr., Sect. D*, *62*, 678–682.

Hedin, L., and S. Lundqvist (1969), Effects of electron-electron and electron-phonon interactions on the one-electron states of solids, *Solid State Phys.*, *23*, 1–181.

Ingalls, A. E., C. Lee, and E. R. M. Druffel (2003), Preservation of organic matter in mound-forming coral skeletons, *Geochim. Cosmochim. Acta*, *67*, 2827–2841.

Levi-Kalisman, Y., S. Raz, S. Weiner, L. Addadi, and I. Sagi (2002), Structural differences between biogenic amorphous calcium carbonate phases using X-ray absorption spectroscopy, *Adv. Funct. Mater.*, *12*, 43–48, doi:10.1002/1616-3028 (20020101)12:1<43::AID-ADFM43>3.0.CO;2-C.

Maslen, E. N., V. A. Streltsov, and N. R. Streltsova (1995), Electron density and optical anisotropy in rhombohedral carbonates. 3. Synchrotron X-ray studies of $CaCO_3$, $MgCO_3$ and $MnCO_3$., *Acta Crystallogr., Sect. B*, *51*, 929–939.

McCulloch, M. T., A. W. Tudhope, T. M. Esat, G. E. Mortimer, J. Chappell, B. Pillans, A. R. Chivas, and A. Omura (1996), Coral record of equatorial sea-surface temperatures during the penultimate deglaciation at Huon Peninsula, *Science*, *283*, 202–204.

Meibom, A., J.-P. Cuif, F. Hillion, B. R. Constantz, A. Juillet-Leclerc, Y. Dauphin, T. Watanabe, and R. B. Dunbar (2004), Distribution of magnesium in coral skeleton, *Geophys. Res. Lett.*, *31*, L23306, doi:10.1029/2004GL021313.

Mitsuguchi, T., E. Matsumoto, O. Abe, T. Uchida, and P. J. Isdale (1996), Mg/Ca thermometry in coral skeletons, *Science*, *274*, 961–963.

Puverel, S., E. Tambutté, L. Pereira-Mouriès, D. Zoccola, D. Allemand, and S. Tambutté (2005), Soluble organic matrix of two Scleractinian corals: Partial and comparative analysis, *Comp. Biochem. Phys., B, Biochem. Mol. Biol.*, *141*, 480–487.

Quinn, T. M., and D. E. Sampson (2002), A multiproxy approach to reconstructing sea surface conditions using coral skeleton geochemistry, *Paleoceanography*, *17*(4), 1062, doi:10.1029/2000PA000528.

Sinclair, D. J., L. P. J. Kinsley, and M. T. McCulloch (1998), High resolution analysis of trace elements in corals by laser ablation ICP-MS, *Geochim. Cosmochim. Acta*, *62*(1), 889–1901.

Suzuki, Y., P. E. D. Morgan, and K. Niihara (1998), Use of a high X-ray flux instrument for a mineral: X-ray powder diffraction pattern of $CaMg(CO_3)_2$, *Powder Diffr.*, *13*, 216–221.

Tambutte, E., D. Allemand, D. Zoccola, A. Meibom, S. Lotto, N. Caminiti, and S. Tambutte (2007), Observations of the tissue-skeleton interface in the scleractinian coral Stylophora pistillata, *Coral Reefs*, *26*, 517–529.

von Barth, U., and L. Hedin (1972), A local exchange-correlation potential for the spin polarized case: I, *J. Phys. C*, *5*, 1629–1642.

Wong, J., G. N. George, I. J. Pickering, Z. U. Rek, M. Rowen, T. Tanaka, G. H. Via, B. De Vries, D. E. W. Vaughan, and G. E. Brown Jr. (1994), New opportunities in XAFS investigation in the 1-2-keV region, *Solid State Commun.*, *92*, 559–562.

Yoshida, T., T. Tanaka, H. Yoshida, T. Funabiki, and S. Yoshida (1995), Study of the dehydration of magnesium hydroxide, *J. Phys. Chem.*, *99*, 10,890–10,896.

N. Allison and A. A. Finch, School of Geography and Geosciences, University of St. Andrews, Irvine Building, St Andrews, Fife KY16 9AL, UK.